Temperature Dependence of Oxygen Reduction Activity at Nafion-Coated Bulk Pt and Pt/Carbon Black Catalysts

Hiroshi Yano,[†] Eiji Higuchi,[†] Hiroyuki Uchida,[‡] and Masahiro Watanabe*,[†]

Clean Energy Research Center, University of Yamanashi, Takeda 4, Kofu 400-8510, Japan, and Interdisciplinary Graduate School of Medicine and Engineering, University of Yamanashi, Takeda 4, Kofu 400-8511, Japan

Received: June 6, 2006; In Final Form: July 3, 2006

Oxygen reduction reaction (ORR) activity and H_2O_2 formation at Nafion-coated film electrodes of bulk-Pt and Pt nanoparticles dispersed on carbon black (Pt/CB) were investigated in 0.1 M $HClO_4$ solution at 30 to 110 °C by using a channel flow double electrode method. We have found that the apparent rate constants k_{app} (per real Pt active surface area) for the ORR at bulk-Pt (with and without Nafion-coating) and Nafion-coated Pt/CB (19.3 and 46.7 wt % Pt, $d_{Pt} = 2.6$ to 2.7 nm) thin-film electrodes were in beautiful agreement with each other in the operation conditions of polymer electrolyte fuel cells (PEFCs), i.e., 30−110 °C and ca. 0.7 to 0.8 V vs RHE. The H_2O_2 yield was 0.6−1.0% at 0.7−0.8 V on all Nafion-coated Pt/CB and bulk-Pt and irrespective of Pt-loading level and temperature. Nafion coating was pointed out to be a major factor for the H_2O_2 formation on Pt catalysts modifying the surface property, because H_2O_2 production was not detected at the bulk-Pt electrode without Nafion coating.

1. Introduction

Polymer electrolyte fuel cells (PEFCs) have been developed intensively as a primary power source for electric vehicles or residences. A typical electrocatalyst layer consists of Pt nanoparticles dispersed on high surface area carbon black (denoted as Pt/CB) coated with perfluorosulfonated ionomer (such as Nafion) as the proton conducting network. The hydrogen oxidation reaction (HOR) overpotential at the anode is negligibly small even at a high current density of 1 A/cm^2 when operated with pure hydrogen. However, a sluggish oxygen reduction reaction (ORR) causes a large cathodic overpotential, i.e., about 80% of the overall loss in the cell. It is, therefore, very important to develop a high performance cathode catalyst.

At the first screening for the electrocatalyst, planar electrodes with well-defined characteristics (active surface area, surface and bulk compositions, and crystal structure) have often been examined in aqueous acidic electrolyte solutions. Use of the rotating disk electrode (RDE) has a great advantage to eliminate a mass-transfer problem and evaluate precisely a kinetically controlled ORR activity.[1−9] The rotating ring-disk electrode (RRDE) provides additional important information on the byproduct H_2O_2, which may deteriorate the polymer electrolyte membrane or gaskets. Schmidt et al. proposed the use of RDE or RRDE to evaluate activities of Pt/CB.[3,4] Commercial Pt/CB (20 wt % Pt/Vulcan XC72) powder was attached onto a glassy carbon (GC) disk electrode by means of a thin Nafion film (ca. 0.05 μm in thickness). Thus, the ORR has been studied with RRDE or RDE at Pt or Pt-alloy electrodes of planar polycrystalline, single crystals, and supported nanoparticles at around room temperature.[1−9] However, even for pure Pt, conflicting results have been reported on the ORR activities and H_2O_2 yields [$P(H_2O_2)$], suggesting the presence of differences in the electrochemical properties between bulk and supported nanoparticles. Such discrepancies have been explained by, for example, so-called "particle-size effect", electronic effect, or morphological (facet exposed or interparticle distance) effect.[10,11] Changes in the local electronic density of states at the Fermi level with Pt particle size were observed by ^{195}Pt NMR.[12]

It must be noted that the ORR activity and the $P(H_2O_2)$ at Pt/CB have not been measured precisely over the wide temperature range practically used in PEFCs: the low-temperature operation is a distinctive feature for portable electronic devices, but higher temperature operation ≥100 °C becomes essential for fuel cell vehicles or residential co-generation systems to achieve a higher conversion efficiency or a higher power density with a low Pt catalyst loading. Regarding the temperature dependencies of the ORR activities as well as $P(H_2O_2)$, there has been little systematic research,[4−7,13−19] because it is difficult to correct the change in the oxygen concentration in the electrolyte solution in the RRDE cell opened to the atmosphere at the elevated temperature.

Recently, we demonstrated that an apparent rate constant k_{app} and apparent activation energy ϵ_a for the ORR at pure Pt and Pt-alloy (Pt−Fe, Pt−Co, and Pt−Ni) electrodes can be precisely evaluated at 20 to 90 °C by using a channel flow double electrode (CFDE) cell.[20,21] The CFDE cell can be operated as a closed system under the controlled oxygen concentration. From the hydrodynamic voltammograms under various laminar flow rates of the O_2-saturated electrolyte solution, the kinetically controlled ORR activity at the planar working electrode can be evaluated. At the collecting electrode located downstream of the working electrode, $P(H_2O_2)$ can be quantified.

In the present paper, we first present interesting results on the temperature dependence of activities [k_{app} for the ORR and $P(H_2O_2)$] at Pt/CB in 0.1 M $HClO_4$ solution at 30−110 °C by the CFDE method, in which Pt/CB powder was attached onto a gold electrode uniformly, followed by coating a thin Nafion

* Author to whom correspondence should be addressed. Phone: +81-55-220-8620. Fax: +81-55-254-0371. E-mail: m-watanabe@yamanashi.ac.jp.
[†] Clean Energy Research Center.
[‡] Interdisciplinary Graduate School of Medicine and Engineering.

10.1021/jp063497t CCC: $33.50
Published on Web 08/02/2006

TABLE 1: Typical Properties of Commercial Pt/CB Catalysts and Preparation Conditions of Catalyst Suspensions and Resulting m_{Pt} and m_{CB} by Pipetting the Suspension with 12.5 μL/cm^2 on Au

catalyst no.	Pt loading[a] (wt %)	d_{Pt}[b] (nm)	$C_{Pt/CB}$[c] (g/L)	m_{Pt}[d] (μg/cm^2)	m_{CB}[e] (μg/cm^2)
1	46.7	2.6	0.82	4.78	5.46
2	19.3	2.7	0.54	1.30	5.45
3	19.3	2.7	1.08	2.60	10.9

[a] Pt weight percent in Pt/CB catalysts. [b] Average diameter of Pt particle estimated by XRD. [c] Amount of Pt/CB catalyst in the suspension. [d] Amount of Pt attached in the catalyst layer. [e] Amount of CB attached in the catalyst layer.

film with the optimized recipe developed by us.[22] We demonstrate that the k_{app} (per real active surface area) for the ORR at Nafion-coated Pt/CB (19.3 and 46.7 wt % Pt, $d_{Pt} = 2.6$ to 2.7 nm) thin-film electrodes is the very same as that of bulk Pt (with and without Nafion-coating) in the whole temperature range and at the practical potential range. The $P(H_2O_2)$ at Nafion-coated Pt/CB and Nafion-coated Pt-bulk are also the same irrespective of the Pt-loading level and temperature (0.6% at 0.80 V and 1.0% at 0.70 V), whereas the H_2O_2 production was not detected at the Pt-bulk electrode without Nafion coating.

2. Experimental Section

Details of the experimental setup of the channel flow double electrode cell and the flow circuit of the electrolyte solution are described in our previous papers.[20,21] The CFDE cell was made of Kel-F blocks and a Teflon sheet, resistant to hot acid electrolyte solution. The substrates for both working and collecting electrodes were mirror-finished gold plates (flow direction length 0.1 cm $\times$ width 0.4 cm, geometric area $A = 0.04$ cm^2), which were inactive for the ORR at a practical potential region more positive than 0.5 V. As the collecting electrode to detect H_2O_2, platinum film was deposited on the gold substrate (downstream side) by DC-sputtering a Pt target at room temperature (SH-33D, ULVAC Co. Ltd.). The working electrodes examined were a bulk-Pt film with and without Nafion coating, Nafion-coated Pt/CB thin films, and Nafion-coated CB (without Pt) thin film. These will be denoted as Pt-(bulk), Nafion-Pt(bulk), Nafion-Pt/CB, and Nafion-CB, respectively. The Pt(bulk) working electrode was prepared in the same manner as that of the collecting electrode. The thickness of the Pt film was controlled to about 0.1 μm.

Platinum-dispersed high-surface-area carbon black catalysts (Pt/CB, Tanaka Kikinzoku Kougyo Co, Ltd.) with Pt-loading of 19.3 wt % (TEC10E20E) and 46.7 wt % (TEC10E50E) were used as-received. As shown in Table 1, the average diameter of Pt estimated by XRD was 2.6 to 2.7 nm, almost independent of the Pt loading. To make ultrathin and uniform dispersion of Pt/CB on the gold substrate, we just modified our previous recipe optimized for Pt/CB on GC disk.[22] The preparation conditions employed are summarized in Table 1. Here, for example, we explain the procedure for the case of No. 1 in Table 1. Pt/CB (4.1 mg; 46.7 wt % Pt-loading) powder was ultrasonically dispersed in 5 mL of ethanol (99.5%) for 20 min ($C_{Pt/CB} = 0.82$ g L^{-1}) by using an ultrasonic homogenizer (US-300T, Nihon Seiki Seisakujo Co. Ltd.). A 0.5 μL aliquot of the suspension was pipetted onto the mirror-finished gold substrate ($A = 0.04$ cm^2, 12.5 μL/cm^2), giving $m_{Pt} = 4.78$ μg/cm^2 and $m_{CB} = 5.46$ μg/cm^2. This was dried at room temperature in a glass Petri dish containing 99.5% ethanol. The dish was covered by a lid with a small gap to evaporate the solvent droplet slowly (for about 3 h) under the saturated vapor pressure of ethanol. Then, 0.5 μL of 0.2 wt % Nafion (diluted with ethanol and water at 3:2 vol %) solution was put on top of the dried catalyst layer to yield the film thickness of 0.1 μm. This was dried at room temperature and under ethanol vapor pressure in the similar manner as described above. Finally, Nafion-Pt/CB on the gold was heat-treated at 130 °C for 30 min in air. As shown in Figure 1, we confirmed uniform dispersion of the catalyst layer over the whole surface with a laser microscope (VK9510, Keyence Co. Ltd.). The major framework (or volume) in the Pt/CB layer is constructed by the CB support, considering the density of CB (2 g/cm^3) and Pt (21.4 g/cm^3). Assuming the uniform catalyst dispersion, the thickness of the CB framework at $m_{CB} = 5.46$ μg/cm^2 is calculated to be 27 nm, which is almost the monolayer height of CB particles. The thickness of the Nafion film for both Pt(bulk) and Pt/CB was controlled to be 0.1 μm in the average thickness, which is thinner than the critical value reported for the ORR.[22] In a similar manner, the Nafion-CB (without Pt, $m_{CB} = 5.46$ μg/cm^2) layer was prepared for comparison purposes.

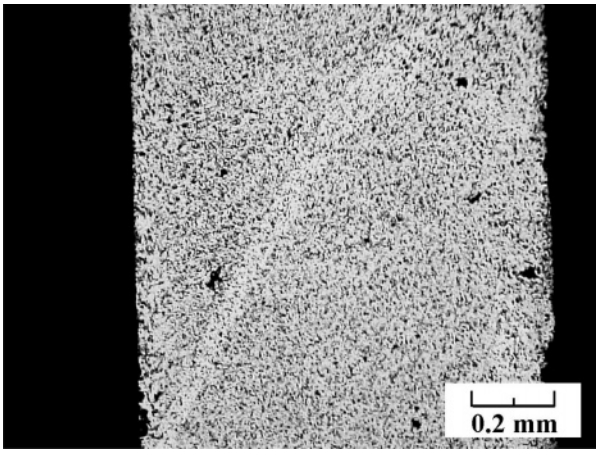

Figure 1. Optical microscope photograph of Pt/CB layer on Au substrate after drying sample No. 1 in Table 1. Well-dispersed CB aggregates (black spots) can be seen.

A Pt wire was used as a counter electrode. The reversible hydrogen electrode kept at the same temperature as that of the cell (t, °C) [denoted as RHE(t)] was used as the reference electrode.[20,21,23] The electrolyte solution of 0.1 M $HClO_4$ was prepared from reagent grade chemicals (Kanto Chemical Co.) and Milli-Q water (Milli-Pore Japan Co. Ltd.) and purified in advance with conventional pre-electrolysis methods.[24−26] The electrolyte solution was saturated with O_2 or N_2 gas bubbling for at least 1 h prior to electrochemical measurements. The total pressure of the gas phase in the electrolyte solution reservoir was controlled with O_2 at 1.0 atm at 30 to 60 °C and 1.5 atm at 70 to 110 °C during the ORR measurements. The oxygen concentration [O_2] and the diffusion coefficient D were calculated based on Henry's law and the Stokes−Einstein equation, respectively (see the Appendix in ref 20).

A bi-potentiostat (ALS 700B, BAS Inc.) was used for the CFDE measurement. Hydrodynamic voltammograms at the working electrode under a flow of O_2-saturated 0.1 M $HClO_4$ solution (mean flow rate $U_m = 10-50$ cm s^{-1}) were recorded by scanning its potential from 0.3 to 1.0 V vs RHE(t) at 0.5 mV s^{-1}. To detect H_2O_2 emitted from the working electrode, the potential of the collecting electrode was set at 1.2 V vs RHE-(t) where H_2O_2 was oxidized under a diffusion-control condition. The collection efficiency (N) for the present CFDE system was experimentally determined to be 0.26 ± 0.01 for all the working

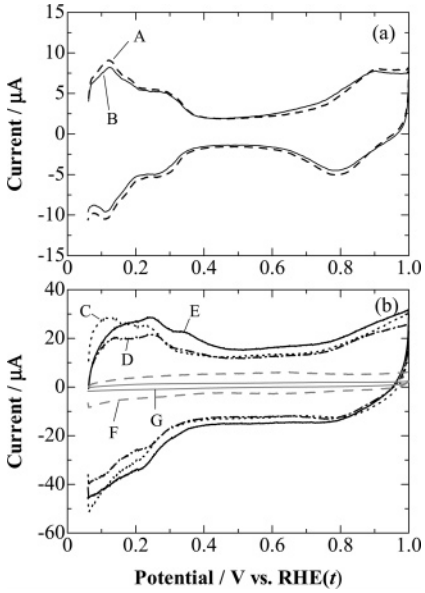

Figure 2. Cyclic voltammograms to determine the roughness factor R_f at (a) Pt(bulk) electrode without (A) and with (B) Nafion-coating and (b) Nafion-Pt(46.7 wt %)/CB with $m_{Pt} = 4.78\ \mu g/cm^2$ (curve C), Nafion-Pt(19.3 wt %)/CB with $m_{Pt} = 1.30\ \mu g/cm^2$ (D), Nafion-Pt(19.3 wt %)/CB with $m_{Pt} = 2.60\ \mu g/cm^2$ (E), Nafion-CB (F), and Au (G) electrodes in N_2 saturated 0.1 M $HClO_4$ solution at 30 °C. Potential scan rate = 0.1 V s^{-1}.

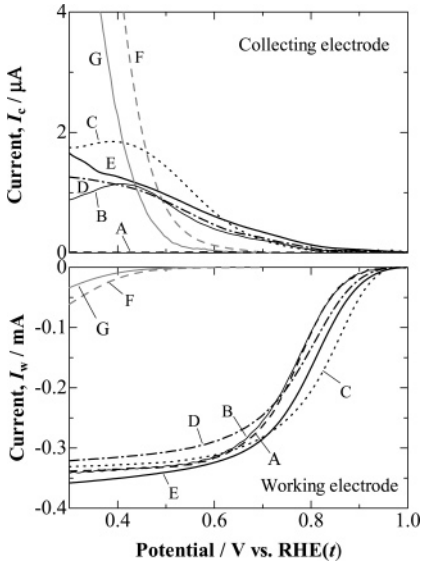

Figure 3. Hydrodynamic voltammograms for the ORR in O_2 saturated 0.1 M $HClO_4$ solution at Pt(bulk) (A), Nafion-coated Pt(bulk) (B), Nafion-Pt(46.7 wt %)/CB with $m_{Pt} = 4.78\ \mu g/cm^2$ (C), Nafion-Pt(19.3 wt %)/CB with $m_{Pt} = 1.30\ \mu g/cm^2$ (D), Nafion-Pt(19.3 wt %)/CB with $m_{Pt} = 2.60\ \mu g/cm^2$ (E), Nafion-CB (F), and Au (G) electrodes at 30 °C and simultaneously acquired currents (I_c) at Pt collecting electrodes for the oxidation of H_2O_2 (by-produced at the working electrodes). Potential scan rate = 0.5 mV s^{-1}. Potential of the collecting electrode = 1.2 V. Mean flow rate of electrolyte $U_m = 50$ cm s^{-1}.

electrodes by using 1 mM $Fe_2(SO_4)_3$ + 0.5 M H_2SO_4 solution. During heating to a desired temperature, the potential of the working electrode was kept at 1.0 V vs RHE(t).

3. Results and Discussion

3.1. Electrochemically Active Area of Bulk Pt, Nafion-Coated Pt, and Pt/CB. Figure 2 shows typical examples of cyclic voltammograms (CVs) at various working electrodes without solution flow in deaerated 0.1 M $HClO_4$ solution at 30 °C. In Figure 2a, the hydrogen adsorption/desorption charge at the Nafion-Pt(bulk) electrode decreases by about 10% compared with the Pt(bulk) (without Nafion) electrode, which is consistent with the literature.[27−30] This reduction is probably due to a specific adsorption of sulfonate groups in Nafion, as observed by in situ FTIR.[31] As shown in Figure 2b, the shape of the CV at Nafion-Pt/CB is similar to that of Pt(bulk), and a noticeable change in the shape is not seen among Pt/CB with 19.3 and 46.7 wt % Pt. In contrast, the Nafion-CB electrode exhibits only a capacitive voltammogram, and the Au substrate (without any film) exhibited a well-known feature of polycrystalline gold.

The electrochemically active surface area S was evaluated from an electric charge of hydrogen desorption wave ΔQ_H in each CV, supposing $\Delta Q_H^\circ = 0.21$ mC/cm^2 for a smooth polycrystalline Pt, as conventionally used.[24,25] The values of apparent roughness factor R_f (ratio of S to geometric surface area A) at 30 °C were 2.7 [Pt(bulk)], 2.4 [Nafion-Pt(bulk)], 2.9 [Nafion-Pt(19.3 wt %)/CB, $m_{Pt} = 1.30\ \mu g/cm^2$], 5.5 [Nafion-Pt(19.3 wt %)/CB, $m_{Pt} = 2.60\ \mu g/cm^2$], and 5.6 [Nafion-Pt-(46.7 wt %)/CB, $m_{Pt} = 4.78\ \mu g/cm^2$).

3.2. Hydrodynamic Voltammetry for ORR. Figure 3 shows hydrodynamic voltammograms for the ORR at various working electrodes in O_2 saturated 0.1 M $HClO_4$ solution at 30 °C at a mean solution flow rate of 50 cm/s and simultaneously acquired currents at the Pt collecting electrode. The ORR currents at the Pt(bulk), Nafion-Pt(bulk), and Nafion-Pt/CB electrodes commence to increase at about 0.95 V vs RHE(30 °C) and reach the limiting currents beyond 0.6 V. Emission of H_2O_2 from the Pt(bulk) working electrode is always below the detection limit (I_c < ca. 10 nA) at the whole temperature range and the potential range of the working electrode. However, small oxidation currents of H_2O_2 at the collecting electrodes are observed for both Nafion-Pt(bulk) and Nafion-Pt/CB. No noticeable ORR currents were detected on Nafion-CB or Au(substrate) at the potential region more positive than 0.6 V. Therefore, we can neglect the contribution of such currents on CB or Au supports in the discussion of the ORR activity at any type of Pt catalyst at $E \geq 0.7$ V.

Then, we discuss in detail the H_2O_2 yield, $P(H_2O_2)$, defined as the percentage of H_2O_2 production rate to that of the overall ORR,

$$P(H_2O_2) = 2I_c/(N \times I_w + I_c) \times 100\% \qquad (1)$$

where I_w and I_c are the currents at the working and collecting electrodes, respectively. As shown in Figure 4, the value of $P(H_2O_2)$ at Nafion-Pt/CB is almost the same as that of Nafion-Pt(bulk) within experimental error for all the conditions (Pt-loading, m_{Pt}, temperature, and potential). The $P(H_2O_2)$ increases slightly with lowering the potential, i.e., 0.6%, 0.7%, and 1.0% at 0.80, 0.76, and 0.70 V, respectively, and is almost independent of the temperature from 50 to 110 °C. In contrast, Nafion-CB and Au(substrate) produce H_2O_2 with $P(H_2O_2) = 98\%$ only at less positive potential region E < 0.65 V, where the two-electron reduction pathway becomes predominant. We inspected the H_2O_2 formation rate at Nafion-CB and Au(substrate) carefully. It was found at 0.70 V and 30−50 °C that the value of I_c detected for Nafion-CB and Au(substrate) working electrodes was less than the detection limit (<ca. 10 nA), corresponding to $P(H_2O_2)$ < 0.05%. Hence, the contribution of Nafion-CB and Au(substrate) to $P(H_2O_2)$ shown in Figure 4 is, if any, very small. Considering $P(H_2O_2) = 0$ at Pt(bulk) (without Nafion), the Nafion coating on Pt is the major reason for triggering H_2O_2

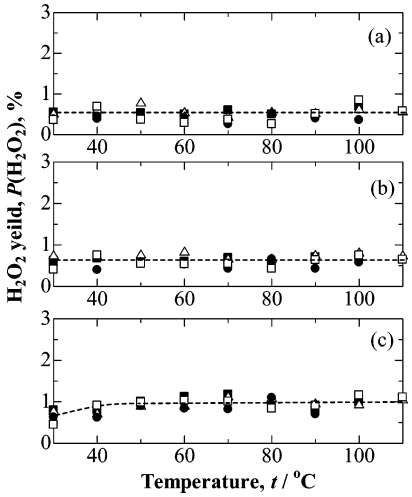

Figure 4. Temperature dependence of H_2O_2 yield at (●) Nafion-Pt-(bulk), (△) Nafion-Pt(46.7 wt %)/CB with $m_{Pt} = 4.78$ μg/cm^2, (□) Nafion-Pt(19.3 wt %)/CB with $m_{Pt} = 2.60$ μg/cm^2, and (■) Nafion-Pt(19.3 wt %)/CB with $m_{Pt} = 1.30$ μg/cm^2 electrodes calculated by using eq 1. The potential of working electrode (V vs RHE(t)) was (a) 0.80, (b) 0.76, and (c) 0.70 V. $U_m = 50$ cm s^{-1}.

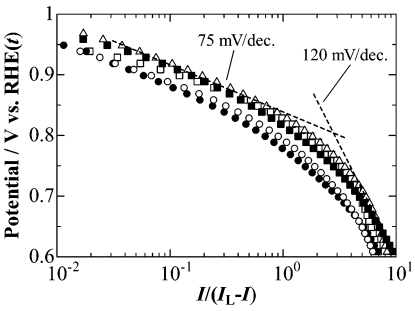

Figure 5. Tafel plots for the ORR at (○) Pt(bulk), (●) Nafion-Pt-(bulk), (△) Nafion-Pt(46.7 wt %)/CB with $m_{Pt} = 4.78$ μg/cm^2, (□) Nafion-Pt(19.3 wt %)/CB with $m_{Pt} = 2.60$ μg/cm^2, and (■) Nafion-Pt(19.3 wt %)/CB with $m_{Pt} = 1.30$ μg/cm^2 electrodes at 70 °C obtained from hydrodynamic voltammograms for ORR in O_2 saturated 0.1 M $HClO_4$ solution. $U_m = 50$ cm s^{-1}.

production at a practical potential region more positive than 0.70 V. It was proposed that the H_2O_2 production on Pt was induced in the presence of strongly adsorbed species such as organic adsorbates or halide anions, which may block the dissociation of adsorbed O_2.[3,21,32,33] Sulfonate groups in Nafion could be possible species strongly adsorbed on the Pt surface in the present case, because the molar concentration of SO_3^- in Nafion corresponds to ca. 1.8 M calculated from the ion exchange capacity (0.91 mmol/g) and the density (2 g/cm^3). Such a specific adsorption of SO_3^- on Pt(bulk) electrode was observed by in situ FTIR.[31] It is clearly shown that the values of $P(H_2O_2)$ are not affected by the Pt-loading level on CB or the amount of Pt attached (m_{Pt}) on the Au substrate over the whole temperature region between 30 and 110 °C. The present result is inconsistent with that claimed from RRDE experiments by Inaba et al.[34] and Zawodzinski et al.,[35] in which the $P(H_2O_2)$ at Nafion-coated Pt/CB on GC at room temperature decreased with increased Pt-loading on CB or the m_{Pt} on the GC. One of the reasons for such a discrepancy is that the amount of CB in their catalyst layers attached on the GC substrate was very high, giving a stacked multilayer, whereas CB in the present work is almost the monolayer height. If the utilization of the catalyst for the ORR was different at the top and bottom of the stacked

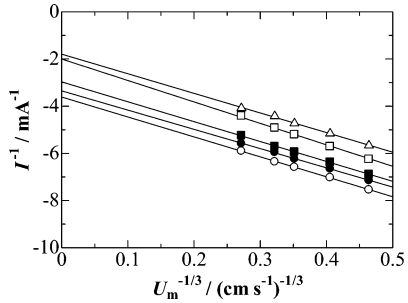

Figure 6. I^{-1} vs $U_m^{-1/3}$ plots obtained from hydrodynamic voltammograms for the ORR at (○) Pt(bulk), (●) Nafion-Pt(bulk), (△) Nafion-Pt(46.7 wt %)/CB with $m_{Pt} = 4.78$ μg/cm^2, (□) Nafion-Pt(19.3 wt %)/CB with $m_{Pt} = 2.60$ μg/cm^2, and (■) Nafion-Pt(19.3 wt %)/CB with $m_{Pt} = 1.30$ μg/cm^2 electrodes at 30 °C and −0.525 V vs $E°$.

layer, the chemical decomposition rate of H_2O_2 could be changed at the position or the thickness, resulting in various $P(H_2O_2)$ values. We point out that such a morphological effect should be discussed separately from the intrinsic property of the Pt catalyst itself. Another possibility to increase the H_2O_2 formation must be a trace amount of impurity species in the electrolyte solution.[3,21,32,33] In all our works, the electrolyte solution carefully purified with conventional pre-electrolysis methods has been used. Thus, we conclude that the H_2O_2 yield $P(H_2O_2)$ on the Nafion-coated Pt is constant and not affected by the morphology such as bulky or nanosized dispersion on a support, the Pt-loading level on supports such as CB or Au at the operating temperature (30−110 °C), and the practical potential (≥0.7 V). We will discuss the effect of Pt-loading on the rate constant for the ORR in the next section.

Figure 5 shows Tafel plots [E vs $\log\{I/(I_L - I)\}$] for the ORR at various electrodes at 70 °C, where I_L is the limiting current. The Tafel slopes at Nafion-Pt(bulk) and Nafion-Pt/CB are similar to that at Pt(bulk), i.e., at ca. −75 mV/decade in the high potential region and ca. −120 mV/decade in the low potential region, respectively, being in agreement with those reported in the literature.[4−7,16−18,36] This suggests that the rate determining step (rds) for the ORR is unchanged at all the Pt-based electrodes, presumably the first electron transfer.

3.3. ORR Activity. The kinetically controlled current I_K at a given potential E is determined from the hydrodynamic voltammogram in the CFDE by using the following equation[37]

$$1/I = 1/I_K + 1/I_L = 1/I_K + 1/\{1.165 \times nF[O_2]w(U_m D^2 x_1^2/h)^{1/3}\} \quad (2)$$

where n is the number of electrons transferred, F is the Faraday constant, $[O_2]$ is the O_2 concentration in the bulk of electrolyte solution, w is the width of the working electrode, U_m is the mean flow rate of the electrolyte solution, D is the diffusion coefficient of O_2, x_1 is the length of the working electrode in the electrolyte flow direction, and h is the half channel height (or half the thickness of the electrolyte flow over the electrodes). Figure 6 shows plots of I^{-1} vs $U_m^{-1/3}$ obtained at 0.76 V vs RHE at 30 °C. Linear relationships are seen at all the electrodes. By extrapolating $U_m^{-1/3}$ to 0 (infinite flow rate), the value of I_K at utilized Pt was determined. As we reported previously, the value of I_K is dependent on the change in the $[O_2]$, which decreases with elevating the operation temperature.[20] Since the contribution of two-electron reduction to produce H_2O_2 to the overall ORR was very low (see Figure 4), we can calculate an apparent rate constant k_{app} at a constant overpotential η from the standard potential $E°$ ($\eta = E - E°$) over the whole operating

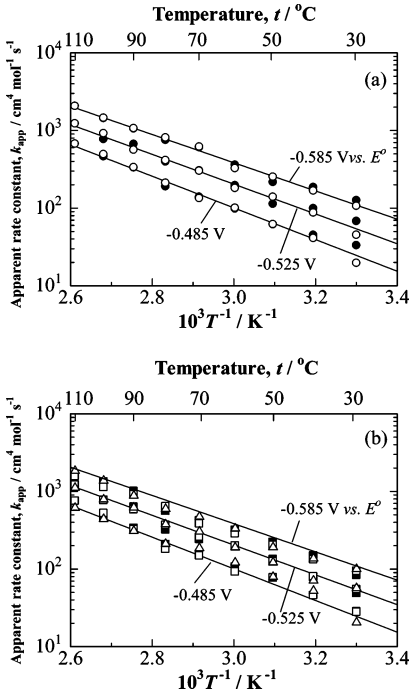

Figure 7. (a) Arrhenius plots of apparent rate constant k_{app} for the ORR at (○) Pt(bulk) and (●) Nafion-Pt(bulk). (b) Arrhenius plots of k_{app} for (△) Nafion-Pt(46.7 wt %)/CB with $m_{Pt} = 4.78$ μg/cm^2, (■) Nafion-Pt(19.3 wt %)/CB with $m_{Pt} = 1.30$ μg/cm^2, and (□) Nafion-Pt(19.3 wt %)/CB with $m_{Pt} = 2.60$ μg/cm^2 electrodes. Solid lines in parts a and b indicate the least-squares fitting of the data for Pt(bulk) and Nafion-Pt(bulk). The overpotential of −0.485, −0.525, and −0.585 V vs $E°$ corresponds to 0.80, 0.76, and 0.70 V vs RHE at 30 °C, respectively.

temperature region from 30 to 110 °C, in the same manner as our previous works,[20,21]

$$I_K/(4FS) = -k_{app}[H^+][O_2] \quad (3)$$

where $[H^+]$ is the bulk concentration of H^+ (0.1 M) and S is the active area of Pt, electrochemically determined with CV in the above section.

Figure 7 shows Arrhenius plots for the k_{app} per real surface area at various electrodes. Since both the $E°$ and E[RHE(t)] shift to less positive values in a different manner, the corrected potential E is applied so as to keep a constant overpotential for the ORR at each temperature.[20] Linear relationships between log k_{app} and $1/T$ are observed at all the electrodes. It is very striking that the values of k_{app} at three kinds of Nafion-Pt/CB electrodes beautifully agree with those of Pt(bulk) with and without Nafion coating in the whole temperature range at a practical potential range. Also, the Pt-loading level on CB or the amount of Pt on the Au substrate provides no effect on the k_{app} among Nafion-Pt/CB electrodes. This is the first demonstration of such important experimental results. In contrast, Paulus et al.[4] reported that the kinetically controlled current densities (per real surface area) for the ORR at Nafion-Pt/CB film were lower than those at bulk polycrystalline Pt at 60 °C in O_2-saturated 0.5 M H_2SO_4, i.e., 190 μA/cm^2 (20 wt % Pt/Vulcan XC 72) vs 400 μA/cm^2 [Pt(bulk)] at 0.85 V. Such a noticeable reduction of the activity should be ascribed to their stacked multilayer (ca. 10 monolayers) of Pt/CB catalysts in their evaluation. Hence, it is essential for the evaluation of the true activity of electrocatalysts supported on CB to disperse them uniformly as in our experimental procedure.

It is also found that, at −0.525 V vs $E°$, the k_{app} values for both bulk Pt and Nafion-coated Pt/CB at 60 and 110 °C are 5 and 35 times higher than that at 30 °C, respectively. This clearly shows the possibility of significant reduction of Pt/CB catalyst loading in PEFCs by such factors by elevating the operating temperature, if the catalyst layer could properly be designed to supply sufficient oxygen to Pt active sites.

Apparent activation energies ϵ_a for the ORR were calculated to be 38, 37, and 36 kJ mol^{-1} on all catalysts at −0.485, −0.525, and −0.585 V vs $E°$, respectively, which are comparable to those on the Pt(bulk) electrode.[20] Thus, we, for the first time, have evaluated the ϵ_a for the ORR at Nafion-Pt/CB together with Nafion-Pt(bulk) under the overpotential keeping constant with the appropriate correction of the change in $[O_2]$ in the whole temperature range.

4. Conclusions

By using the CFDE method, we have obtained crucial results that the ORR activities and the H_2O_2 formation rates at Pt/CB with different loading levels of Pt (19.3 and 46.7 wt %, with almost the same d_{Pt} of 2.6 nm) on CB support and Pt/CB on Au support, in comparison with a planar bulk-Pt electrode in O_2-saturated 0.1 M $HClO_4$ solution at 30 to 110 °C and an operation potential range, $E > 0.7$ V. We first have found that the apparent ORR rate constants at all of Nafion-Pt/CB agree quite well with those of Pt(bulk) with and without Nafion coating in the whole temperature range at $E > 0.7$ V. The same apparent activation energy (37 kJ mol^{-1} at $\eta = -0.525$ V) was seen at all of Nafion-Pt/CB, Nafion-Pt(bulk), and Pt(bulk). A small amount of H_2O_2 formation was observed at both Nafion-Pt(bulk) and Nafion-Pt/CB electrodes [$P(H_2O_2)$ = ca. 0.6%, 0.7%, and 1.0% at the potential of 0.80, 0.76, and 0.70 V between 50 and 110 °C, respectively]. The value of $P(H_2O_2)$ was independent of the Pt-loading on CB and the amount of Pt on the Au substrate. In contrast, emission of H_2O_2 from the Pt(bulk) working electrode without Nafion coating was always below the detection limit at the whole temperature and the potential range of the working electrode. Therefore, the Nafion coating on Pt(bulk) brought about the enhancement of H_2O_2 formation, indicating that sulfonate groups in Nafion strongly adsorb on Pt sites and modify the surface property, which may suppress the dissociation of adsorbed O_2 on Pt active sites.

Acknowledgment. This work was supported by the fund for "Leading Project" of the Ministry of Education, Science, Culture, Sports and Technology of Japan.

References and Notes

(1) Watanabe, M.; Igarashi, H.; Yoshioka, K. *Electrochim. Acta* **1995**, *40*, 329.

(2) Markovic, N. M.; Schmidt, T. J.; Stamenkovic, V.; Ross, P. N. *Fuel Cell* **2001**, *1*, *105*.

(3) Schmidt, T. J.; Paulus, U. A.; Gasteiger, H. A.; Behm, R. J. *J. Electroanal. Chem.* **2001**, *508*, 41.

(4) Paulus, U. A.; Schmidt, T. J.; Gasteiger, H. A.; Behm, R. J. *J. Electroanal. Chem.* **2001**, *495*, 134.

(5) Grgur, B. N.; Markovic, N. M.; Ross, P. N. *Can. J. Chem.* **1997**, *75*, 1465.

(6) Markovic, N. M.; Adzic, R. R.; Cahan, B. D.; Yeager, E. *J. Electroanal. Chem.* **1994**, *377*, 249.

(7) Yeager, E.; Razaq M.; Gervasio, D.; Razaq, A.; Tryk, D. In *Structural Effects in Electrocatalysis and Oxygen Electrochemistry*, PV 92-11; Scherson, D., et al., Eds.; The Electrochemistry Society: Pennington, NJ, 1992; p 440.

(8) Paulus, U. A.; Wokuanu, A.; Schmidt, T. J.; Stamenkovic, V.; Radmilovic, V.; Markovic, N. M.; Ross, P. N. *J. Phys. Chem. B* **2002**, *106*, 4181.

(9) Paffett, M. T.; Beery, J. G.; Gottesfeld, S. *J. Electrochem. Soc.* **1988**, *135*, 1431.

(10) Chen, S.; Kucernak, A. *J. Phys. Chem. B* **2004**, *108*, 3262.

(11) Giordano, N.; Passalacqua, E.; Pino, L.; Arico, A. S.; Antonucci, V.; Vivaldi, M.; Kinoshita, K. *Electrochim. Acta* **1991**, *36*, 1979.
(12) Rice, C.; Tong, Y.; Oldfield, E.; Wieckowski, A. *Electrochim. Acta* **1998**, *43*, 2825.
(13) Beattie, P. D.; Basura, V. I.; Holdcroft, S. *J. Electroanal. Chem.* **1999**, *468*, 180.
(14) Enayetullah, M. A.; DeVilbiss, T. D.; Bockris, J. O'M. *J. Electrochem. Soc.* **1989**, *136*, 3369.
(15) Scharifker, B. R.; Zelenay, P.; Bockris, J. O'M. *J. Electrochem. Soc.* **1987**, *134*, 2714.
(16) Sepa, D. B.; Vojnovic, M. V.; Vracar, Lj. M.; Damjanovic, A. *Electrochim. Acta* **1986**, *31*, 91.
(17) Sepa, D. B.; Vojnovic, M. V.; Vracar, Lj. M.; Damjanovic, A. *Electrochim. Acta* **1986**, *31*, 97.
(18) Damjanovic, A.; Sepa, D. B. *Electrochim. Acta* **1990**, *35*, 1157.
(19) Toda, T.; Honma, I. *Trans. Mater. Res. Soc. Jpn.* **2003**, *288*, 215.
(20) Wakabayashi, N.; Takeichi, M.; Itagaki, M.; Uchida, H.; Watanabe, M. *J. Electroanal. Chem.* **2005**, *574*, 339.
(21) Wakabayashi, N.; Takeichi, M.; Uchida, H.; Watanabe, M. *J. Phys. Chem. B* **2005**, *109*, 5836.
(22) Higuchi, E.; Uchida, H.; Watanabe, M. *J. Electroanal. Chem.* **2005**, *583*, 69.
(23) Wakabayashi, N.; Uchida, H.; Takeuchi, K.; Watanabe, M. *Electrochem. Solid-State Lett.* **2002**, *5*, E62.
(24) Watanabe, M.; Motoo, S. *J. Electroanal. Chem.* **1975**, *60*, 275.
(25) Watanabe, M.; Motoo, S. *J. Electroanal. Chem.* **1975**, *60*, 259.
(26) Uchida, H.; Ikeda, N.; Watanabe, M. *J. Electroanal. Chem.* **1997**, *424*, 5.
(27) Lawson, D. R.; Whiteley, L. D.; Martin, C. R. *J. Electrochem. Soc.* **1988**, *135*, 2247.
(28) Zecevic, S. K.; Wainright, J. S.; Litt, M. H.; Gojkovic, S. L.; Savinell, R. F. *J. Electrochem. Soc.* **1997**, *144*, 2973.
(29) Chu, D.; Tryk, D.; Gervasio, D.; Yeager, E. B. *J. Electroanal. Chem.* **1989**, *272*, 277.
(30) Chu, D. *Electrochim. Acta* **1998**, *43*, 3711.
(31) Ayato, Y.; Kunimatsu, K.; Osawa, M.; Okada, T. *J. Electrochem. Soc.* **2006**, *153*, A203.
(32) Markovic, N.; Gasteiger, H.; Ross, P. N. *J. Electrochem. Soc.* **1997**, *144*, 1591.
(33) Stamenkovic, V.; Markovic, N. M.; Ross, P. N., Jr. *J. Electroanal. Chem.* **2001**, *500*, 44.
(34) Inaba, M.; Yamada, H.; Tokunaga, J.; Tasaka, A. *Electrochem. Solid-State Lett.* **2004**, *7*, A474.
(35) Agarwal, A. S.; Karuppaiah, C.; Landau, U.; Zawodzinski, T. The 206th Meeting of The Electrochemical Society, Honolulu, Hawaii, 2004, Abstract 1896.
(36) Stamenkovic, V.; Schmid, T. J.; Ross, P. N.; Markovic, N. M. *J. Electroanal. Chem.* **2003**, *554*, 191.
(37) Levich, V. G. In *Physicochemical Hydrodynamics*; Prentice Hall: Englewood Cliffs, NJ, 1962; p 112.